Article

Carbon nanotube-polyamidoamine dendrimer hybrid-modified electrodes for highly sensitive electrochemical detection of microRNA24

Fengye Li, Jing Peng, Qiong Zheng, Xiang Guo, Hao Tang, and Shouzhuo Yao

Anal. Chem., **Just Accepted Manuscript** • DOI: 10.1021/acs.analchem.5b00093 • Publication Date (Web): 15 Apr 2015

Carbon nanotube-polyamidoamine dendrimer hybrid-modified electrodes for highly sensitive electrochemical detection of microRNA24

Fengye Li[1,‡], Jing Peng[1,‡], Qiong Zheng[1,‡], Xiang Guo[1], Hao Tang[1,*], Shouzhuo Yao[2]

[1]Key Laboratory of Chemical Biology and Traditional Chinese Medicine Research (Ministry of Education), College of Chemistry and Chemical Engineering, Hunan Normal University, Changsha 410081, P.R. China.

[2]State Key Laboratory of Chemo/Biosensing and Chemometrics, Hunan University, Changsha 410082, P.R. China.

ABSTRACT: A simple and ultrasensitive microRNA (miRNA) electrochemical biosensor employing multi-walled carbon nanotube (MWCNT)-polyamidoamine (PAMAM) dendrimer and methylene blue (MB) redox indicator is reported in this work. The assay utilizes a glass carbon (GC) electrode modified with MWCNT-PAMAM, on which the oligonucleotide capture probes are immobilized. The electrochemical detection of miRNAs is completed by measuring the reduction signal change of MB before and after the probe hybridization with target miRNA (miRNA24 is used as a model case). The MWCNT-PAMAM/GC electrode shows greatly enhanced signal to MB reduction in contrast to bare GC electrode. The functionalization of MWCNT with PAMAM maintains the electrochemical property of MWCNT to MB reduction but minimizes the undesired adsorption of MB on the MWCNT surface. The effect of experimental variables on the miRNA detection is investigated and optimized. A detection limit of 0.5 fM and a linear peak current density-concentration relationship up to 100 nM are obtained following 60-min hybridization. The proposed assay is successfully used to detect miRNA24 in total RNA sample extracted from HeLa cells.

The study on the microRNA (miRNA) biology has obtained tremendous attentions in the past decade because more and more evidence demonstrate that miRNA dysregulation could lead to a large number of genetic diseases [1-2]. The miRNA expression profiles are associated with the pathogenesis of most human malignancies and may serve as biomarkers for cancer diagnosis, prognosis, and therapy [3-7]. These provide powerful impetus and a growing demand for scientific researchers to establish an accurate and sensitive analytical methodology for miRNA detection. Although the intrinsic characteristics of miRNAs make their expression profiling with sensitivity and specificity extremely challenging, several well-established detection tools have been developed and reviewed in the literatures [8-10]. The reverse-transcription polymerase chain reaction (RT-PCR) and northern blot methods are the most common used in early reports and the gold standard in determination of miRNAs [11-12]. Quantitative PCR technique using stem-loop primers and locked nucleic acid is also becoming a popular way for miRNA detection due to its high level of sensitivity and specificity [13-14]. To support the high-throughput characterization of miRNA expression profiles, microarray chips have been developed [15]. By integration of PCR for target amplification and the labeling of products, it has demonstrated to improve the analytical performances and cost-effectiveness of microarray chips. These conventional technologies have intrinsic advantages along with some limitations. In addition to the conventional methods, optical detection technologies including fluorescence [16], bioluminescence [17], surface-enhanced Roman spectroscopy [18-19], and surface plasmon resonance imaging [20] have found their way into the realm of miRNA expression profiling in recent years. These optical technologies have demonstrated to address the shortcoming associated with the conventional methods, for example, increasing multiplexing capability, selectivity, and dynamic range while decreasing sample size, cost, and turnaround time.

Electrochemical assays offer highly attractive perspectives for miniaturized, smaller, faster, and cheaper devices, which are desirable for point-of care and make them great potential in miRNA determination. Various strategies based on different electrochemical transducing methods have been employed for miRNA analysis. The used electrochemical transducing methods include amperometry, voltammetry, conductometry, impedimetry, and potentiometry [10]. As representatives, the isoniazid-capped OsO_2 nanoparticles [21], streptavidin-coated paramagnetic beads [22], and graphene-dendritic gold nanostructures [23] have been utilized to construct amperometric miRNA biosensors with excellent analytical performances. Voltammetry has also been proved to be another useful electrochemical transducing method for miRNA detection [24]. The silver nanoclusters [25] and Nafion-thionin-Pd nanoparticle hybrids [26] with excellent metal mimic enzyme property for catalyzing H_2O_2 reduction show enhancement of the current response of the voltammetric miRNA biosensors. The biotinylated miRNAs, which can bind to the extravidin labeled alkaline phosphatase [27] or streptavidin-ferrocene-capped gold nanoparticles conjugates [28], have been utilized to complete sensitive miRNA detection. Other unique approaches, for example, a three-mode voltammetric miRNA sensor, utilizing hybridization, p19 protein binding, and protein displacement, have been reported [29]. This p19 protein displacement-based sensor can be theoretically employed for detection of any type of miRNAs by using one kind of thiolated capture probe and as low as 5 aM of target miRNA can be identified with high selectivity and specificity. The RNA-binding p19 protein was also used as a selective bio-recognition element to develop a magnetobiosensor [30], being able to detect 0.4 fM of miRNA21 in 2 h in total RNA

extracted from cancer cells and human breast-tumor specimens without PCR amplification and sample pre-processing. Moreover, the multiplexed chip shows highly sensitivity for miRNA detection, allowing directly analysis of nanograms of total RNA within 30 min [31].

The voltammetric miRNA biosensors described above allow rapid, sensitive, and highly specific miRNA determination. However, it usually involves chemical/biological labeling, enzymatic reactions, or expensive and special probes, which make the electrochemical assays relatively complicated. Simpler and cheaper voltammetric miRNA biosensors with high sensitivity and good selectivity are highly desirable for uses at point-of-care. The electrochemical DNA biosensors have been intensively investigated and successfully used in the past decades. Moreover, most present methods for miRNA detection are relied on the hybridization between a target miRNA and a complementary DNA probe to produce a double-stranded helical molecule. Therefore, the principles for electrochemical DNA detection should be applicable for electrochemical miRNA assays. Electrochemical redox indictors, being capable of binding with different affinity to single stranded (ss) and double stranded (ds) DNA, are continuing to be of particular interest for electrochemical analysis of DNA sequences because the use of hybridization indicators allows the development of simple and cost-effective biosensor platform. The phenothiazine dye Methylene Blue (MB) is possibly one of the most popular redox indicators. The different affinity of MB for ss and dsDNA nucleic acid sequences and selectivity of MB electrochemistry to mismatches in the hybrids allow the application of MB as an excellent redox indicator in a variety of electrochemical DNA assays [32-34].

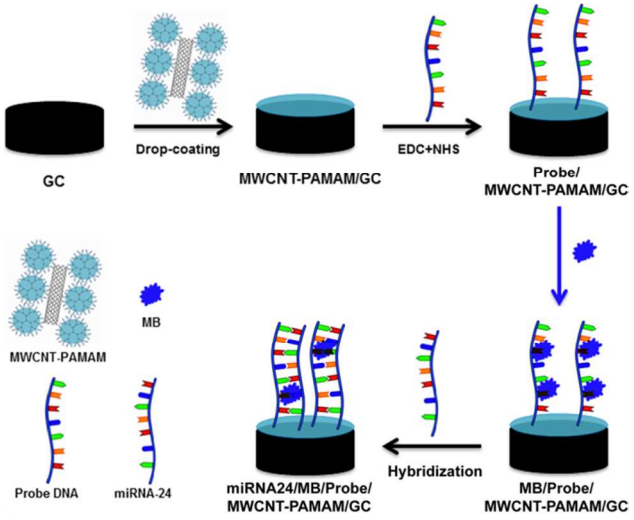

Figure 1. Schemes demonstrating the principle of miRNA24 electrochemical biosensor based on the MWCNT-PAMAM hybrids.

Recently, dual signal amplification strategy based on the catalyzed hairpin assembly reaction and hybridization chain reaction was introduced to develop an electrochemical miRNA biosensor using MB as indicator [35]. Besides hybridization signal amplification, in itself, the capture probe DNA immobilization and the electrochemical property of the electrode for MB signal transducing should be key points for fabrication of electrochemical miRNA biosensors with high performances. In this work, the multi-walled carbon nanotube (MWCNT)-polyamidoamine (PAMAM) dendrimer hybrids were proposed to construct a simple, label-free, and sensitive electrochemical miRNA biosensor using MB as indicator (Figure 1). The electrochemical detection of miRNAs is based on the MB reduction consequent to the hybridization between the target miRNA and the complementary DNA capture probe. The reduction of MB before and after hybrid formation generates voltammetric signal change, which is measured by differential pulse voltammetry (DPV). The unique chemical and physical properties of MWCNTs have paved the way to new and improved sensing devices, in general, and electrochemical biosensors, in particular [36-37]. MWCNTs have excellent electrochemical property for MB electrochemistry, already described for studying the dsDNA-MB interaction [38-39]. On the other hand, PAMAM dendrimers are a unique class of high branched polymeric macromolecules, which possess numerous peripheral groups. For example, the number of peripheral amine groups of each PAMAM (generation 4.0) molecule reaches 64, being very suitable for immobilization of capture probe [40]. The use of MWCNT-PAMAM hybrids may enhance the immobilization of capture DNA and the sensitivity of MB measurements, resulting in improved analytical performance for electrochemical detection of miRNAs. Moreover, in contrast to the existing miRNA detection schemes, which exploit labeled DNA sequences, enzyme reactions, or special probe DNA, the application of MB indicator removes the cumbersome and relatively expensive steps of chemical/biological labeling or enzyme reactions. This will simplify the analysis and reduce its price, making the proposed miRNA biosensor attractive. As a model case, we used the miRNA24, which plays important roles in cell proliferation [41-42] and cancer cell differentiation [43]. The proposed MWCNT-PAMAM-based biosensor exhibits good analytical properties (high sensitivity, low detection limit, good selectivity, reproducibility, and regeneration property) for miRNA24 detection.

EXPERIMENTAL SECTION

Chemicals and Instruments. The used MWCNTs and chemicals were listed in Supporting Information. The synthetic 5'-carboxyl group terminated DNA capture probe, miRNA24, central single base-mismatched miRNA24, and miRNA29 were obtained from Invitrogen Corporation (Life Technologies, Shanghai). The base sequences of the DNA capture probe and miRNAs are as follows:

DNA probe 5'-HOOC-C TGT TCC TGC TGA ACT GAG CCA-3'

miRNA24 5'-UGG CUC AGU UCA GCA GGA ACA G-3'

Central single base-mismatched miRNA24 5'-UGG CUC AGU UGA GCA GGA ACA G-3'

miRNA29 5'-UAG CAC CAU CUG AAA UCG GUU A-3'

The total RNA sample was extracted from cultured human cervical cancer (HeLa) cells by TRIZOL reagents (Invitrogen Corporation, Life Technologies, Shanghai) according to the manufacturer's recommended protocol. The quality of total RNA was routinely assessed by gel electrophoresis (1% gelose, 80 V, 20 min) and BioPhotometer plus (Eppendorf). The 5S rRNA, 18S rRNA, and 28S rRNA bands were all clear in electrophoresis picture (Figure S1, Supporting Information) and the OD_{260}/OD_{280} was larger than 1.8 (the results not shown), indicating that high quality and intact RNA was extracted from the samples [44]. The total RNA concentration was measured by UV-vis spectrophotometry. HeLa cells were obtained from Cancer Research Institute of Xiangya Medical College.

UltraPure™ diethyl pyrocarbonate (DEPC)-treated water was purchased from Invitrogen Corporation (Life Technologies, Shanghai) and was used for miRNA24 determination and the preparation of total RNA sample solution (1.2 μg μL^{-1}). Phosphate buffered saline (PBS, 0.1 M, pH 7.38) solutions were used in the experiments. Sodium citrate for preparation of saline-sodium citrate (SSC) solutions, sodium dodecyl sulfate (SDS), and all other reagents were of analytical grade or better. Milli-Q ultrapure water (> 18 MΩ cm, Milli-pore Co., Ltd.) and fresh prepared solutions were used throughout.

The instruments for electrochemical measurements were presented in Supporting Information. The experiments were performed at room temperature. The electrochemical measurements were repeated at least three times. The means of the measurements were presented with the standard deviations (SD).

Preparation of MWCNT-PAMAM modified GC electrode and capture probe immobilization. The received MWCNTs were chemically oxidized by the mixed acids (concentrate H_2SO_4+HNO_3, v/v 3:1) for 24 h to prepare the carboxylated MWCNTs. The details are according to the previous work [45]. The MWCNT aqueous suspension (1.0 mg mL^{-1}) was prepared for future use (hereafter, unless otherwise specified, the MWCNTs were referred to the carboxylated MWCNTs). The details for preparation of the MWCNT-PAMAM hybrids [46], the MWCNTs/glass carbon (GC, 3 mm diameter) and MWCNT-PAMAM/GC electrodes, and the immobilization of capture probes on the MWCNT-PAMAM/GC electrode were presented in Supporting Information.

Electrochemical measurements. The electrochemical behavior of MB at the MWCNT-PAMAM/GC electrode was investigated by DPV in PBS solutions containing MB (1.0 mM) and the details were presented in Supporting Information.

For the miRNA24 hybridization and electrochemical detection, the probe/MWCNT-PAMAM/GC electrode prepared was dipped into 5 mL of PBS solutions containing 60 μM MB for 10 min, followed by rinse with PBS and DEPC water three times. The hybridization reaction was completed by dipping the MB/probe/MWCNT-PAMAM/GC electrode into 100 μL of DEPC water containing different concentration of miRNA24 for 1 h at room temperature. After successive washing with 1× SSC, 0.1% SDS, and DEPC water in turn for 2 min, the MB electrochemical reduction signal of the miRNA24/MB/probe/MWCNT-PAMAM/GC electrode was measured by DPV in blank PBS over the potential range of 0.1 to -0.6 V. The DPV parameters are as follows: potential increment, 4 mV; amplitude, 50 mV; pulse period, 0.2 s. The MB reduction signal of the MB/probe/MWCNT-PAMAM/GC electrode was also measured as the background. The procedures are the same as the miRNA24/MB/probe/MWCNT-PAMAM/GC electrode. To test the specificity of the assay, the synthetic oligonucleotides of miRNA29 and the central single base-mismatched miRNA24 were used as control. Moreover, the analytical applicability of the prepared probe/MWCNT-PAMAM/GC electrode in complex sample was evaluated using total RNA sample that extracted from HeLa cells. Briefly, the prepared MB/probe/MWCNT-PAMAM/GC electrode was immersed into 100 μL of DEPC water (99 μL) and total RNA sample solution (1 μL, 1.2 μg μL^{-1}) mixture. After hybridization for 1 h at room temperature and successive washing with 1× SSC, 0.1% SDS, and DEPC water in turn for 2 min, the MB electrochemical reduction signal of the resulting electrode was measured by DPV in blank PBS. The concentration of miRNA24 in total RNA sample solution was calculated according to the calibration curve. For comparison, the miRNA24 in total RNA sample solution was also determined by quantitative PCR technique by ABI Prism® 7500 Sequence Detection System. The SYBR-Green qPCR Super Mix for the determination was obtained from Invitrogen Corporation, Life Technologies (Shanghai).

RESULTS AND DISCUSSION

Electrochemical behavior of MB at the MWCNT-PAMAM/GC electrode

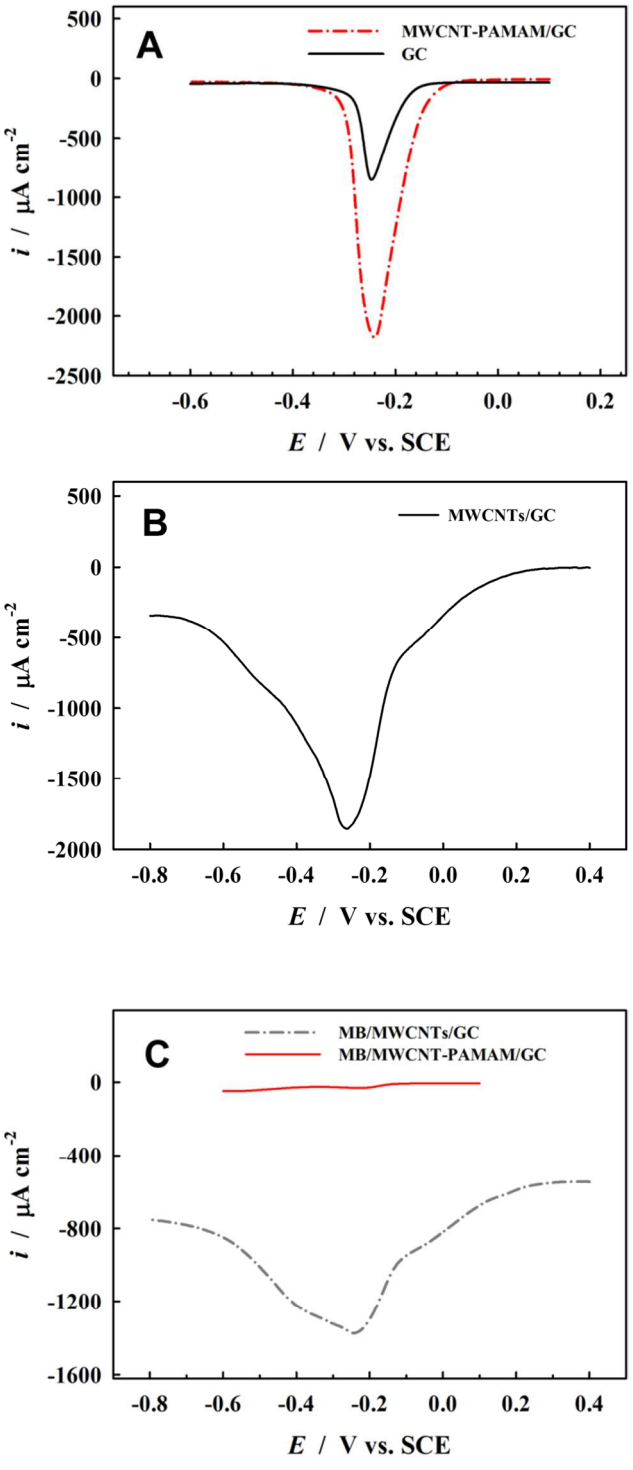

Figure 2. DPV curves of the GC (A, black line), MWCNT-PAMAM/GC (A, red dash-dotted line), and MWCNTs/GC (B, black line) electrodes in PBS (pH 7.38) solutions containing MB. (C) DPV curves of the MWCNTs/GC (gray dash-dotted line) and MWCNT-PAMAM/GC (red line) electrodes in blank PBS; before DPV scanning, the electrodes were immersed into PBS solutions containing MB for 10 min, and then rinsed with PBS three times. The concentration of MB is 1.0 mM and the loading masses of MWCNTs and MWCNT-PAMAM hybrids are all 35.36 μg cm^{-2}.

The electrochemical property of the MWCNT-PAMAM/GC electrode for MB electrochemical reduction was investigated to confirm the feasibility of the MWCNT-PAMAM-based electrochemical biosensor for miRNA24 detection. The DPV curves of MB at the GC and MWCNT-PAMAM/GC electrodes (Figure 2A) demonstrate that well-defined electro-reduction peaks for MB appear at about -0.240 V, being accordant with other works [32, 47]. The cathodic peak current density (i_{peak}) of MB at the bare GC electrode is about 0.78 mA cm^{-2} (Figure 2A, black line). The signal obtained with bare GC electrode is attributed to the adsorption of phenothiazine compounds on electrode surface [32]. The electro-reduction peak potential of MB at the MWCNT-PAMAM/GC electrode is the same with that at the GC electrode, but the i_{peak} of MB electro-reduction reaches 2.17 mA cm^{-2} (Figure 2A, red dash-dotted line), being about 2.8 times as large as that at the GC electrode. The modification of GC electrode with the MWCNT-PAMAM hybrids facilitates larger surface coverage, providing enhanced adsorption of MB, and consequently offers larger i_{peak} of MB electro-reduction. The greatly improved MB reduction signal by using the MWCNT-PAMAM hybrids should promote the analytical performances for miRNA24 detection.

To investigate the effect of PAMAM functionalization on the electrochemical property of the MWCNT-PAMAM/GC electrode for MB electro-reduction, the MWCNTs/GC electrode was prepared and characterized. The MB exhibits a broad reduction peak at the MWCNTs/GC electrode from about 0.2 to -0.7 V. The reduction peak potential at the MWCNTs/GC is about -0.25 V and the i_{peak} is about 1.79 mA cm^{-2} (Figure 2B), suggesting that the tethering of PAMAM dendrimer molecules onto the surface of MWCNTs doesn't degrade the electrochemical property of the MWCNT-PAMAM/GC electrode for MB electron-transfer. More importantly, it seems that the PAMAM functionalization minimizes the undesired adsorption of MB on the MWCNT surface. The MWCNTs/GC and MWCNT-PAMAM/GC electrodes were first immersed into PBS solutions containing 1.0 mM MB for 10 min, followed by rinse with PBS three times, and then measured in blank PBS by DPV (Figure 2C). Large signal, corresponding to the MB reduction, was still observed at the MWCNTs/GC electrode (Figure 2C, gray dash-dotted line), demonstrating that lots of MB remained on the MWCNTs/GC surface after rinse with PBS. But for the MWCNT-PAMAM/GC electrode, the MB reduction i_{peak} was only about 25 μA cm^{-2} (Figure 2C, red line). This may suggest that the interaction of MB with MWCNT-PAMAM hybrids is weaker than that with MWCNTs, and most of the adsorbed MB can be rinsed out from the MWCNT-PAMAM/GC electrode surface. It is known that the adsorption of MB onto MWCNTs is very stable and will be a spontaneous process [48] via π-stacking interaction between MB and MWCNTs [49-50]. In addition, MB is cationic dye and will exist as positively charged ions in aqueous solution [48]. The carboxylated MWCNTs used in this work are negatively charged in the studied pH. Therefore, the electrostatic attraction also benefits for MB adsorption by the MWCNTs. However, the functionalization of PAMAM dendrimers onto MWCNTs may increase the steric hindrance for MB adsorption. Moreover, the primary amine groups of MWCNT-PAMAM hybrids will be positively charged in physiological pH, resulting in electrostatic repulsion between the PAMAM and MB. These factors may be attributed to the decrease of MB adsorption stability. In our work, miRNA24 detection was completed by measuring the reduction i_{peak} change of MB indicator before and after hybridization. The PAMAM dendrimer-modification will not only introduce tremendous amine groups for DNA probe immobilization but also decrease the adsorption stability of MB, which should be favorable to minimize the undesired adsorption of MB on the MWCNT-PAMAM/GC electrode. Therefore, the use of MWCNT-PAMAM/GC electrode will enhance the sensitivity and accuracy of miRNA determination.

DPV characterization of the probe/MWCNT-PAMAM/GC electrode before and after hybridization using MB as an indicator

The electrochemical detection of miRNA24 was performed by DPV transduction of the hybridization between the immobilized capture probe and the target miRNA24 using MB as an indicator. The i_{peak} of MB at the probe/MWCNT-PAMAM/GC electrode is used as background and the change of MB signal (Δi_{peak}) after hybridization thus shows the target miRNA24. The DPV technique provides lower detection limits than the ones obtained by square wave voltammetry and potentiometric stripping analysis [51]. Figure 3 shows the typical DPV curves of the MB/probe/MWCNT-PAMAM/GC electrode before (red line) and after (blue dash-dotted line) hybridization with miRNA24. The MB/probe/MWCNT-PAMAM/GC and miRNA24/MB/probe/ MWCNT-PAMAM/GC electrodes show well-defined signals at about -0.235 V, which is corresponding to the electro-reduction of MB. The reduction i_{peak} of MB after miRNA24 hybridization significantly decreases in contrast to that of the MB/probe/MWCNT-PAMAM/GC electrode and the Δi_{peak} reaches about 254 μA cm^{-2}. It is widely known that MB intercalates with DNA. Two possible mechanism of interaction have been established, by electrostatic interaction with negatively charged backbone phosphate groups or by interaction between guanine bases. MB shows a higher affinity for ssDNA rather than dsDNA, being confirmed by spectroscopy study [32]. Yang et al [52] have reported the evidence of direct interaction of MB with guanine bases. Erdem et al [53-54] have suggested the MB interacts with guanine bases specifically and the hybridization limits the interaction between guanine and MB [32, 53], and therefore, a lower MB reduction current is observed upon DNA hybridization. The decrease of MB reduction signal after hybridization may be due to the different affinity of MB for the ssDNA capture probe and capture DNA-miRNA24 hybrids. To confirm this assumption from electrochemistry, the probe/MWCNT-PAMAM/GC electrode was first hybridized with the target miRNA24. The obtained miRNA24/probe/MWCNT-PAMAM/GC electrode was then immersed into PBS solutions containing MB (20 μM) for 10 min, and after rinsed with PBS three times, the resulting MB/miRNA24/probe/MWCNT-PAMAM/GC electrode was measured in blank PBS. The reduction i_{peak} of MB is almost the same with that of the MB/probe/MWCNT-PAMAM/GC electrode (Figure S2, Supporting Information). If the interaction between guanine base and MB was not limited after formation of the probe DNA-miRNA24 hybrids, the MB signal at

the MB/miRNA24/probe/MWCNT-PAMAM/GC electrode should be larger than that before hybridization (Figure S2, black line, Supporting Information). The positively charged MB would electrostatically interact with the negatively charged backbone phosphates of probe DNA-miRNA24 hybrid. It is obviously that the probe DNA-miRNA24 hybrid has more phosphate groups for MB binding, which should promote the MB signal. The results of Figure S2 (Supporting Information) confirm the proposed assumption from the view of electrochemistry. In addition, the control experiments were also performed to confirm the decrease of MB reduction i_{peak} after hybridization was not because of the rinse steps (Figure S3, Supporting Information). Anyway, based on the above results, it is feasible to detect miRNA24 by the proposed MWCNT-PAMAM-based electrochemical biosensor using MB as redox indicator.

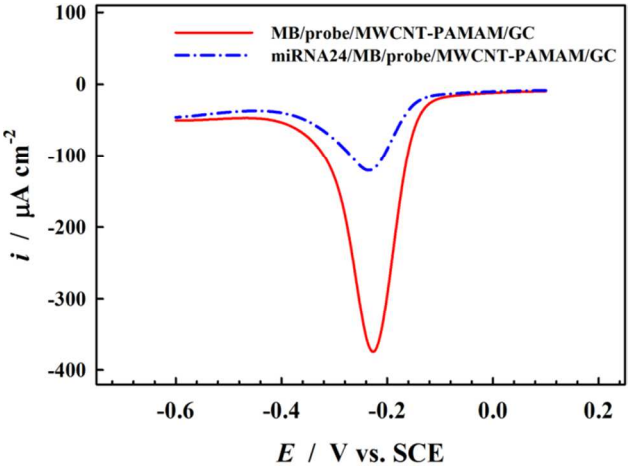

Figure 3. Typical DPV curves of the MB/probe/MWCNT-PAMAM/GC electrodes before (red line) and after (blue dash-dotted line) miRNA24 hybridization. The loading mass of MWCNT-PAMAM is 35.36 μg cm^{-2}; the added volume of the probe solution (1 μM) and the reaction time are 10 μL and 2 h; the MB concentration is 60 μM and the MB adsorption time is 10 min; the concentration of miRNA24 is 0.1 μM and the hybridization time is 1 h.

Optimization of the conditions for miRNA24 electrochemical detection

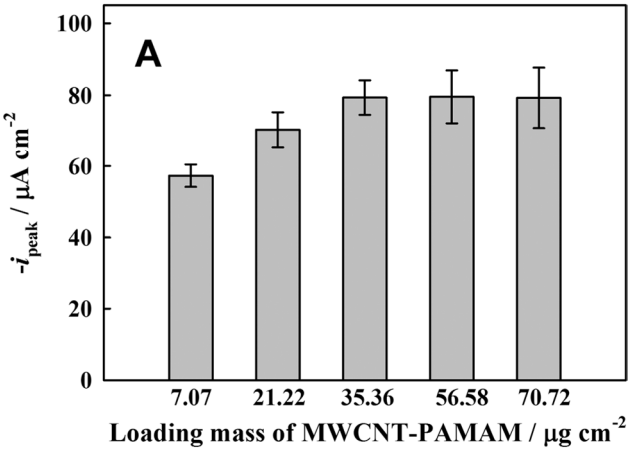

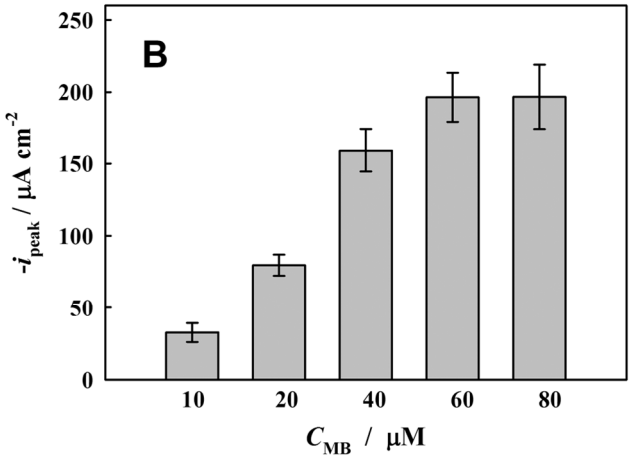

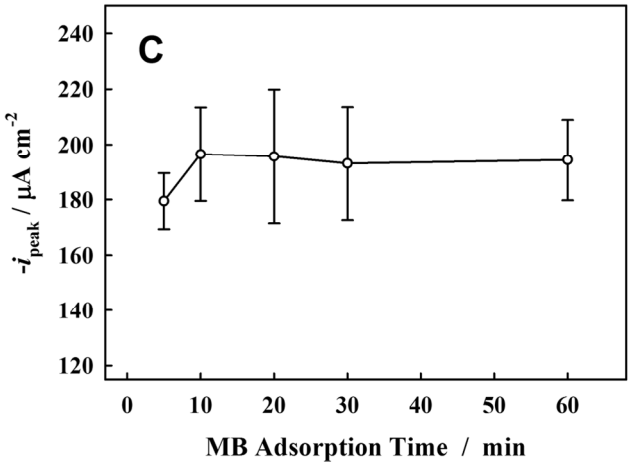

Figure 4. Effects of the MWCNT-PAMAM loading mass (A), MB concentration (B), and MB adsorption time (C) on the i_{peak} of MB electro-reduction at the MB/probe/MWCNT-PAMAM/GC electrodes. The loading mass of MWCNT-PAMAM in B and C is 35.36 μg cm^{-2}; the added volume of the probe solution (1 μM) is 5 μL and the reaction time is 1 h; the MB concentration is 20 μM (A) and 60 μM (C); the MB adsorption time in A and B is 10 min.

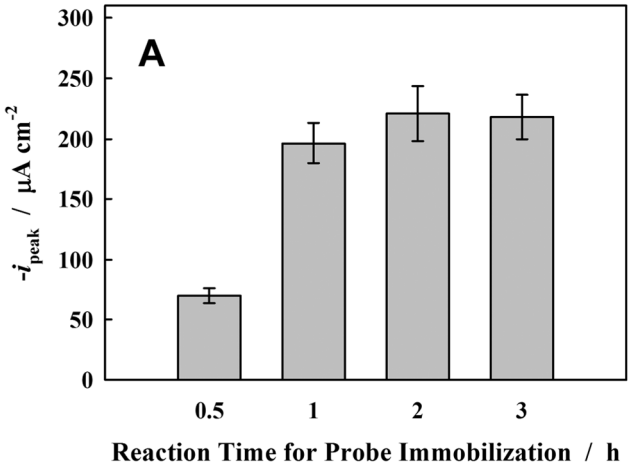

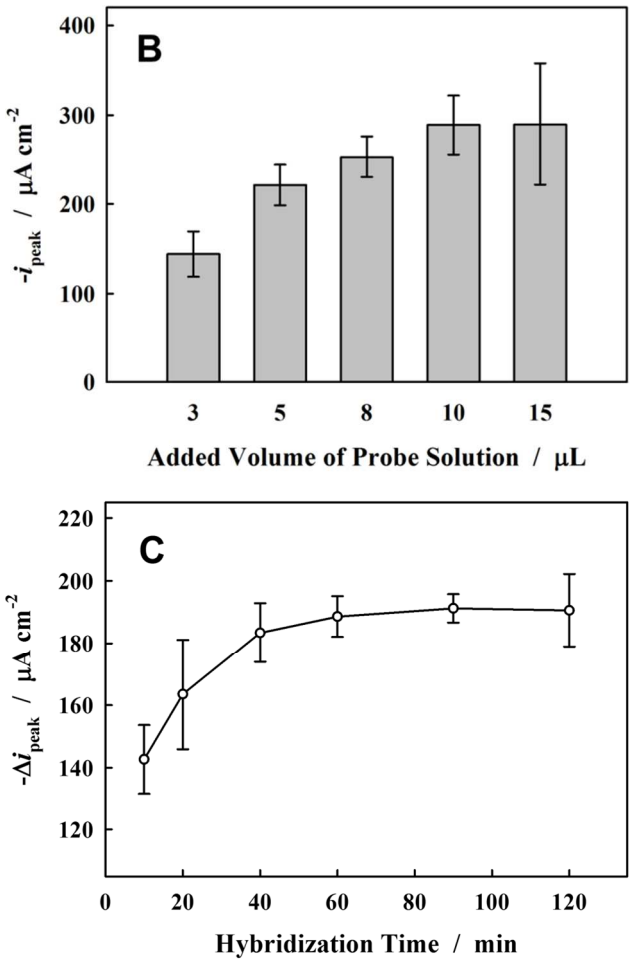

Figure 5. Effects of the reaction time for probe immobilization (A) and the added volume of probe solution (B) on the i_{peak} of MB electro-reduction at the MB/probe/MWCNT-PAMAM/GC electrodes. (C) Dependence of the Δi_{peak} on the miRNA24 hybridization time. The loading mass of MWCNT-PAMAM is 35.36 μg cm^{-2}; the added volume of the probe solution (1 μM) is 5 μL (A) and 10 μL (C); the reaction time for probe immobilization in B and C is 2 h; the MB concentration is 60 μM and the MB adsorption time is 10 min; the concentration of miRNA24 is 0.1 μM.

To obtain optimal conditions for miRNA24 detection, the effects of MWCNT-PAMAM loading mass, MB concentration and adsorption time, reaction time for probe immobilization, adding volume of probe solution, and hybridization time on the i_{peak} of the MB/probe/MWCNT-PAMAM/GC and miRNA24/MB/probe/MWCNT-PAMAM/GC electrodes were investigated in detail. The MB/probe/MWCNT-PAMAM/GC electrode shows the largest i_{peak} at 35.36 μg cm^{-2} of MWCNT-PAMAM loading (Figure 4A). Further increase of MWCNT-PAMAM loading mass doesn't improve the i_{peak} of MB. Too much loading of the MWCNT-PAMAM hybrids will lead to aggregation among the hybrids, and thus the active sites (primary amine groups on the MWCNT-PAMAM surface) for capture probe immobilization will maintain at a maximum value. The MB concentration has significant effect on the i_{peak} of the MB/probe/MWCNT-PAMAM/GC electrodes (Figure 4B). The i_{peak} at 60 μM MB reaches 196 μA cm^{-2}, being about 6 times larger than that at 10 μM MB. In given MB adsorption time (10 min, for example), the increase of MB concentration will facilitate the dynamic interaction of MB with the probe DNA, resulting in the increase of electrochemical response of the MB/probe/MWCNT-PAMAM/GC electrode. When the MB concentration is larger than 60 μM, the MB adsorption reaches saturation, and hence the MB/probe/MWCNT-PAMAM/GC electrode shows maximum response at 60 μM MB. At fixed MB concentration (60 μM), MB exhibits saturation adsorption at the probe/MWCNT-PAMAM/GC electrode in 10 min (Figure 4C). Figure 5A and B shows the effects of reaction time for carboxylated probe DNA activation and the added volume of probe solution. The MB/probe/MWCNT-PAMAM/GC electrode has the largest i_{peak} when the activation time is 2 h and 10 μL of probe solution (1 μM) is added onto the MWCNT-PAMAM/GC electrode. In addition, the effect of hybridization time was also evaluated (Figure 5C). The Δi_{peak} before and after miRNA24 hybridization increases with the increase of hybridization time (10-60 min) and 60 min of hybridization produces the largest Δi_{peak}. In the following experiments, the miRNA24 detections were all performed under the optimal conditions.

Analytical properties of the probe/MWCNT-PAMAM/GC electrode for miRNA24 detection

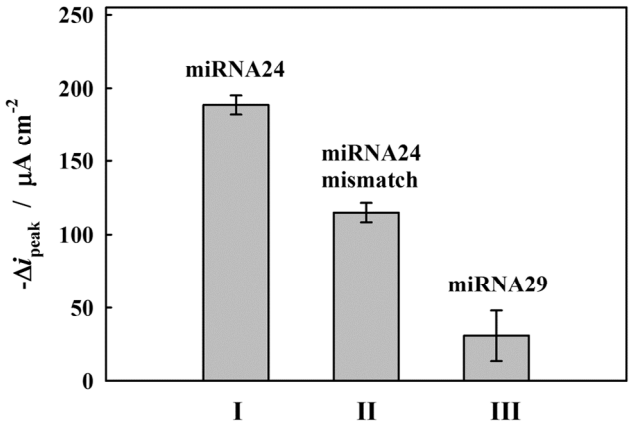

Figure 6. Responses of the MB/probe/MWCNT-PAMAM/GC electrodes to three kinds of miRNAs. The concentrations of the miRNAs are all 0.1 μM.

The central single base-mismatched miRNA-24 and miRNA29 were used as control to test the selectivity of the assay. Figure 6 shows the responses of the MB/probe/MWCNT-PAMAM/GC electrodes to different miRNAs. The Δi_{peak} (31 μA cm^{-2}) obtained from the hybridization with 0.1 μM of miRNA29 (Figure 6 III) is very little in contrast to that (189 μA cm^{-2}) from the miRNA24 (Figure 6, I), suggesting that the assay has good selectivity. Theoretically, the used probe DNA would not hybridize with a non-complementary sequence, and hence the MB signal should not decrease after interaction with miRNA29. However, the nonspecific adsorption of miRNA29 on the MB/probe/MWCNT-PAMAM/GC electrode surface cannot be completely eliminated, although it is effectively suppressed by washing steps using SSC and SDS [55]. The little Δi_{peak} in the presence of miRNA29 should be caused by limited interactions between MB and miRNA29. The Δi_{peak} after hybridization with the central single base-mismatched miRNA24 (Figure 6, II) is about 60% of that after hybridization with miRNA24 (Figure 6, I), suggesting the assay can somewhat discriminate the central single base-mismatch of miRNA24. The mismatched single base is centrally located in the used sequence and half of the sequence could hybridize with

the probe DNA, resulting in relatively large Δi_{peak} response. This result is accordant with that reported in other work [29]. In general, there is very little probability that the miRNA24 and its central single base-mismatched sequence are simultaneously present. The proposed assay will detect miRNA24 from complex sample with good specificity.

The reproducibility of the MB/probe/MWCNT-PAMAM/GC electrode was also evaluated. Samples (0.1 μM) were detected by four MB/probe/MWCNT-PAMAM/GC electrodes prepared under the same conditions, giving a relative standard deviation (RSD) of 6.8%. This reveals that the miRNA24 biosensor has satisfied reproducibility. In addition, the proposed miRNA24 biosensor has good regeneration property and can be used for miRNA24 detection at least four times (Figure S4, Supporting Information). Moreover, the prepared MWCNT-PAMAM/GC and probe/MWCNT-PAMAM/GC electrodes show relatively good storage stability in seven days (Figure S5, Supporting Information).

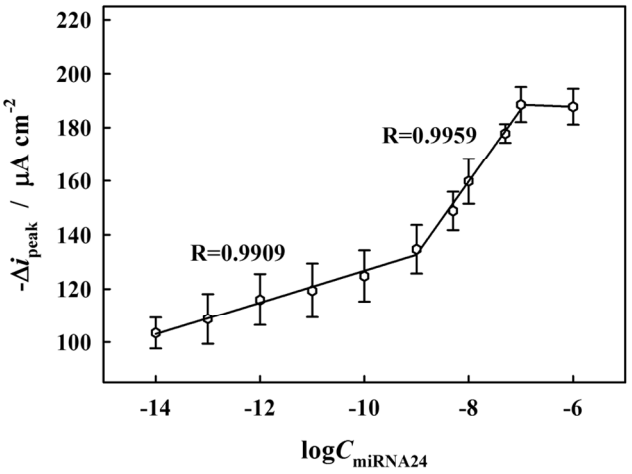

Figure 7. The calibration curve of the prepared MWCNT-PAMAM-based biosensor for miRNA24 detection.

Figure 7 shows the relationship between the Δi_{peak} and the logarithm of miRNA24 concentration ($\log C_{miRNA24}$). The Δi_{peak} - $\log C_{miRNA24}$ curve exhibits two linear ranges with different slopes in the studied concentration range. From 10 fM to 1 nM, the increase of Δi_{peak} with the increase of miRNA24 concentration is not so significant. But the Δi_{peak} exhibits obvious increase with further increase of miRNA24 concentration (1 - 100 nM) and a flat value is observed when 1 μM of the target is used. The Δi_{peak} shows different tendency with the increase of miRNA24 concentration, which is probably due to the hybridization efficiency between the probe DNA and the target [56]. The regression equations in the ranges of 10 fM to 1 nM and 1-100 nM can be obtained and expressed as $\Delta i_{peak}=186.1+5.9\log C_{miRNA24}$ and $\Delta i_{peak}=376.3+27.1\log C_{miRNA24}$. The two linear curves have the slopes of 5.9 and 27.1 μA cm^{-2} $decade^{-1}$ (the sensitivity of the miRNA24 biosensor) and the correlation coefficients are 0.9909 and 0.9959. A detection limit of 0.5 fM for the target miRNA can be estimated using 3σ [34] (where σ is the standard deviation of the blank solution), which is lower than that of the existing works using various voltammetric sensing platform including inosine-substituted capture probes [24], Pd nanoparticles as enhancer and linker [26], enzyme amplified biosensing [27], MWCNTs/GC [56], and is comparable with those reported previously using other protocols with signal amplification for various miRNA voltammetric detection [25, 28, 57]. The detection limits and linear range of several voltammetric biosensors for different miRNA detection are listed in Table S1 (Supporting Information). The analytical applicability of the proposed miRNA24 biosensor was evaluated by determination miRNA24 in the total RNA sample. The concentration of miRNA24 in the total RNA sample solution (extracted from HeLa cells) was found to be 0.0103 μM (n=3, RSD=6.9%), which was comparable with that (0.0110 μM, n=3, RSD=13.9%) obtained from the quantitative PCR detection. The results demonstrate that the proposed MWCNT-PAMAM-based voltammetric biosensor using MB as indicator has good potential for complex miRNA sample detection. Considering the complexity and sequence homology of miRNA family members, however, further detail studies, including determination of different target miRNAs in total RNA samples extracted from various types of cancer cells, are needed for the practical application of the proposed assay in miRNA analysis.

CONCLUSIONS

It is demonstrated that the MWCNT-PAMAM hybrids and MB redox indicator can be used to develop a simple and sensitive electrochemical miRNA biosensor. Under optimal conditions, the prepared probe/MWCNT-PAMAM/GC electrode has good sensitivity, low detection limit, good specificity, regeneration property, and storage stability for miRNA24 determination. In contrast to other miRNA detection protocols, the MWCNT-PAMAM-based biosensor is directly based on the signal change of MB redox indicator, which remove the cumbersome and relatively expensive steps of chemical/biological labeling or enzyme reactions and hence, simplify the analysis and reduce its price. The proposed MWCNT-PAMAM biosensor may find wide applications in the routine detection of miRNAs by a simple way.

ASSOCIATED CONTENT

Supporting Information

The electrophoresis result of the total RNA. The used chemicals and instruments. Details for preparation of the MWCNT-PAMAM hybrids. Pretreatment of the GC electrode and preparation of the MWCNTs/GC and MWCNT-PAMAM/GC electrodes. Details for capture probe DNA immobilization. Electrochemical measurements of MB at the MWCNT-PAMAM/GC electrode. DPV response of the MB/miRNA24/probe/MWCNT-PAMAM/GC electrode. Effect of rinse steps on the MB reduction i_{peak}. Regeneration property of the biosensor. Storage stability of the MWCNT-PAMAM/GC and probe/MWCNT-PAMAM/GC electrodes. Summary of detection limit and linear range of voltammetric miRNA biosensors reported in the literatures. This material is available free of charge via the Internet at http://pubs.acs.org.

AUTHOR INFORMATION

Corresponding Author

* Tel. /Fax: +86-731-88872618. E-mail: tanghao@hunnu.edu.cn.

Author Contributions

The manuscript was written through contributions of all authors. All authors have given approval to the final version of the manuscript. ‡These authors contributed equally.

Notes

The authors declare no competing financial interest.

ACKNOWLEDGMENT

This work was supported by the National Natural Science Foundation of China under grants (21275050, 21145001), the Hunan Provincial Natural Science Foundation of China (13JJ1016), the Scientific Research Fund of Hunan Provincial Education Department (13A053), and the Aid Program for Science and Technology Innovative Research Team in Higher Educational Institutions of Hunan Province.

REFERENCES

(1) Carthew, R. W. *Curr. Opin. Genet. Dev.* **2006**, *16*, 203-208.
(2) Zamore, P. D.; Haley, B. *Science* **2005**, *309*, 1519-1524.
(3) Calin, G. A.; Dumitru, C. D.; Shimizu, M.; Bichi, R.; Zupo, S.; Noch, E.; Aldler, H.; Rattan, S.; Keating, M.; Rai, K.; Rassenti, L.; Kipps, T.; Negrini, M.; Bullrish, F.; Croce, C. M. *Proc. Natl. Acad. Sci. U. S. A.* **2002**, *99*, 15524-15529.
(4) Chan, J. A.; Krichevsky, A. M.; Kosik, K. S. *Cancer Res.* **2005**, *65*, 6029-6033.
(5) Huang, Q.; Gumireddy, K.; Schrier, M.; le Sage, C.; Nagel, R.; Nair, S.; Egan D.A.; Li, A.; Huang, G.; Klein Szanto, A. J.; Gimotty, P. A.; Katsaros, D.; Coukos, G.; Zhang, L.; Pure, E.; Agami, R. *Nat. Cell Biol.* **2008**, *10*, 202-210.
(6) Thum, T.; Gross, C.; Fielder, J.; Fischer, T.; Kissler, S.; Bussen, M.; Galuppo, P.; Just, S.; Rottbauer, W.; Frantz, S.; Castoldi, M.; Soutschek, J.; Koteliansky, V.; Rosenwald, A.; Basson, M. A.; Licht, J. D.; Pena, J. T. R.; Bauersachs, J.; Engelhardt, S. *Nature* **2008**, *456*, 980-984.
(7) Xiao, C.; Rajewsky, K. *Cell* **2009**, *136*, 26-36.
(8) Cissell, K. A.; Deo, S. K. *Anal. Bioanal. Chem.* **2009**, *394*, 1109-1116.
(9) Mariangelsde, P.-S.; Maria, C. R. *Anal. Chim. Acta* **2011**, *699*, 134-152.
(10) Teo, A. K. L.; Lim, C. L.; Gao, Z. Q. *Electrochim. Acta* **2014**, *126*, 19-30.
(11) Shi, R.; Chiang, V. L. *BioTechniques* **2005**, *39*, 519-525.
(12) Yu, Z.; Zhu, Y.; Zhang, Y.; Li, J.; Fang, Q.; Xi, J.; Yao, B. *Talanta* **2011**, *85*, 1760-5.
(13) Chen, C.; Ridzon, D. A.; Broomer, A. J.; Zhou, Z.; Lee, D. H.; Nguyen, J. T.; Barbisin, M.; Xu, N. L.; Mahuvakar, V. R.; Andersen, M. R.; Lao, K. Q.; Livak, K. J.; Guegler, K. J. *Nucleic Acids Res.* **2005**, *33*, e179.
(14) Li, J.; Yao, B.; Huang, H.; Wang, Z.; Sun, C.; Fan, Y.; Chang, Q.; Li, S.; Wang, X.; Xi, J. *Anal. Chem.* **2009**, *81*, 5446-5451.
(15) Draghici, S.; Khatri, P.; Eklund, A. C.; Szallasi, Z. *Trends Genet.* **2006**, *22*, 101-109.
(16) Liang, R.-Q.; Li, W.; Li, Y.; Tan, C.-y.; Li, J.-X.; Jin, Y.-X.; Ruan, K.-C. *Nucleic Acids Res.* **2005**, *33*, e17.
(17) Cissell, K. A.; Rahimi, Y.; Shrestha, S.; Hunt, E. A.; Deo, S. K. *Anal. Chem.* **2008**, *80*, 2319-2325.
(18) Driskell, J. D.; Tripp, R. A. *Chem. Commun.* **2010**, *46*, 3298-3300.
(19) Driskell, J. D.; Seto, A. G.; Jones, L. P.; Jokela, S.; Dluhy, R. A.; Zhao, Y. P.; Tripp, R. A. *Biosens. Bioelectron.* **2008**, *24*, 917-922.
(20) Fang, S.; Lee, H. J.; Wark, A. W.; Corn, R. M. *J. Am. Chem. Soc.* **2006**, *128*, 14044-14046.
(21) Gao, Z.; Yang, Z. *Anal. Chem.* **2006**, *78*, 1470-1477.
(22) Bettazzi, F.; Hamid-Asl, E.; Esposito, C.; Quintavalle, C.; Formisano, N.; Laschi, S.; Catuogno, S.; Iaboni, M.; Marrazza, G.; Mascini, M.; Cerchia, L.; De Franciscis, V.; Condorelli, G.; Palchetti, I. *Anal. Bioanal. Chem.* **2013**, *405*, 1025-1034.
(23) Yin, H.; Zhou, Y.; Zhang, H.; Meng, X.; Ai, S. *Biosens. Bioelectron.* **2012**, *33*, 247-253.
(24) Lusl, E. A.; Passamano, M.; Guarasclo, P.; Scarpa, A.; Schlavo, L. *Anal. Chem.* **2009**, *81*, 2819-22.
(25) Dong, H.; Jin, S.; Ju, H.; Hao, K.; Xu, L.-P.; Lu, H.; Zhang, X. *Anal. Chem.* **2012**, *84*, 8670-8674.
(26) Wu, X.; Chai, Y.; Yuan, R.; Su, H.; Han, J. *Analyst* **2013**, *138*, 1060-1066.
(27) Kilic, T.; Topkaya, S. N.; Ariksoysal, D. O.; Ozsoz, M.; Ballar, P.; Erac, Y.; Gozen, O. *Biosens. Bioelectron.* **2012**, *38*, 195-201.
(28) Wang, J.; Yi, X.; Tang, H.; Han, H.; Wu, M.; Zhou, F. *Anal. Chem.* **2012**, *84*, 6400-6406.
(29) Labib, M.; Khan, N.; Ghobadloo, S. M.; Cheng, J.; Pezacki, J. P.; Berezovski, M. V. *J. Am. Chem. Soc.* **2013**, *135*, 3027-3038.
(30) Campuzano, S.; Torrente-Rodriguez, R. M.; Lopez-Hernandez, E.; Conzuelo, F.; Grannados, R.; Sanchez-Puelles, J. M.; Pingarron, J. M. *Angew. Chem. Int. Ed.* **2014**, *53*, 6168-6171.
(31) Yang, H.; Hui, A.; Pampalakis, G.; Soleymani, L.; Liu, F.-F.; Sargent, E. H.; Kelley, S. O. *Angew. Chem. Int. Ed.* **2009**, *48*, 8461-8464.
(32) Erdem, A.; Kerman, K.; Meric, B.; Ozsoz, M. *Electroanalysis* **2001**, *13*, 219-223.
(33) Boon, E. M.; Ceres, D. M.; Drummond, T. G.; Hill, M. G.; Barton, J. K. *Nat. Biotech.* **2000**, *18*, 1096-1100.
(34) Chen, J.; Zhang, J.; Wang, K.; Lin, X.; Huang, L.; Chen, G. *Anal. Chem.* **2008**, *80*, 8028-8034.
(35) Wu, X. Y.; Chai, Y. Q.; Yuan, R.; Zhuo, Y.; Chen, Y. *Sens. Actuators, B* **2014**, *203*, 296-302.
(36) Wang, J. *Electroanalysis* **2005**, *17*, 7-14.
(37) Elrouby, M. *J. Nanotech. Adv. Mater.* **2013**, *1*, 23-38.
(38) Garcia-Gonzalez, R.; Costa-Garcia, A.; Teresa Fernandez-Abedul, M. *Sens. Actuators, B* **2014**, *202*, 129-136.
(39) Arias, P.; Ferreyra, N. F.; Rivas, G. A.; Bollo, S. *J. Electroanal. Chem.* **2009**, *634*, 123-126.
(40) Benters, R.; Niemeyer, C. M.; Drutschmann, D.; Blohm, D.; Wöhrle, D. *Nucleic Acids Res.* **2002**, *30* (e10), 1-7.
(41) Lagos-Quintana, M.; Rauhut, R.; Lendeckel, W.; Tuschl, T. *Science* **2001**, *294*, 853-858.
(42) Cheng, A. M.; Byrom, M. W.; Shelton, J.; Ford, L. P. *Nucleic Acids Res.* **2005**, *33*, 1290-1297.
(43) Cameron, J. E.; Fewell, C.; Yin, Q.; McBride, J.; Wang, X.; Lin, Z.; Flemington, E. K. *Virology* **2008**, *382*, 257-266.
(44) Sambrook, J.; Fristsch, E. F.; Maniatis, T. Cold Spring Harbor Laboratory Press: Cold Spring Harbor: NY, 2nd ed. edn., 1989.
(45) Li, C.; Yang, K.; Zhang, Y.; Tang, H.; Yan, F.; Tan, L.; Xie, Q.; Yao, S. *Acta Biomater.* **2011**, *7*, 3070-3077.
(46) Liu, X.; Ma, D.; Tang, H.; Tan, L.; Xie, Q.; Zhang, Y.; Ma, M.; Yao, S. *ACS Appl. Mater. Interfaces* **2014**, *6*, 8173-8183.
(47) Kelley, S. O.; Barton, J. K.; Jackson, N. M.; Hill, M. G. *Bioconjugate Chem.* **1997**, *8*, 31-37.
(48) Yao, Y.; Xu, F.; Chen, M.; Xu, Z.; Zhu, Z. *Bioresour. Technol.* **2010**, *101*, 3040-3046.
(49) Yan, Y.; Zhang, M.; Gong, K.; Su, L.; Guo, Z.; Mao, L. *Chem. Mater.* **2005**, *17*, 3457-3463.
(50) Li, Y.; Du, Q.; Liu, T.; Peng, X.; Wang, J.; Sun, J.; Wang, Y.; Wu, S.; Wang, Z.; Xia, Y.; Xia, L. *Chem. Eng. Res. Des.* **2013**, *91*, 361-368.
(51) Palecek, E.; Fojta, M. *Anal. Chem.* **1994**, *66*, 1566-1571.
(52) Yang, W. R.; Ozsoz, M.; Hibbert, D. B.; Gooding, J. J. *Electroanalysis* **2002**, *14*, 1299-1302.
(53) Erdem, A.; Kerman, K.; Meric, B.; Akarca, U. S.; Ozsoz, M. *Anal. Chim. Acta* **2000**, *422*, 139-149.
(54) Erdem, A.; Ozsoz, M. *Anal. Chim. Acta* **2001**, *437*, 107-114.
(55) Ariksoysal, D. O.; Karadeniz, H.; Erdem, A.; Sengonul, A.; Sayiner, A. A.; Ozsoz, M. *Anal. Chem.* **2005**, *77*, 4908-4917.
(56) Li, F.; Peng, J.; Wang, J.; Tang, H.; Tan, L.; Xie, Q.; Yao, S. *Biosens. Bioelectron.* **2014**, *54*, 158-164.
(57) Fan, Y.; Chen, X. T.; Trigg, A. D.; Tung, C. H.; Kong, J. M.; Gao, Z. Q. *J. Am. Chem. Soc.* **2007**, *129*, 5437-5443.

Table of Contents (TOC)